MAJOR PAPER

Diffusion-weighted MR Imaging for the Assessment of Renal Function: Analysis Using Statistical Models Based on Truncated Gaussian and Gamma Distributions

Kentaro Yamada[1], Hiroshi Shinmoto[1*], Koichi Oshio[2], Seigo Ito[3],
Hiroo Kumagai[3], and Tatsumi Kaji[1]

[1]Department of Radiology, National Defense Medical College, Saitama,
3-2 Namiki, Tokorozawa, Saitama 359-0042, Japan
[2]Department of Diagnostic Radiology, Keio University School of Medicine
[3]Department of Nephrology and Endocrinology, National Defense Medical College

Purpose: To determine the appropriateness of statistical models using the truncated Gaussian distribution and gamma distribution for diffusion signal decay, and to assess the correlation between the parameters obtained from the statistical models and estimated glomerular filtration rate (eGFR).

Methods: Twenty-nine patients with chronic kidney disease and 21 healthy volunteers were included and classified in four groups according to eGFR (ml/min/1.73 m^2): group 1 ($90 \leq$ eGFR, n = 10), group 2 (eGFR 60–90, n = 15), group 3 (eGFR 30–60, n = 17), and group 4 (eGFR < 30, n = 8). Diffusion-weighted imaging using five b-values (0, 500, 1000, 1500, and 2000 s/mm^2) was performed. Truncated Gaussian and gamma models were compared for goodness of fit. Area fractions for the diffusion coefficient $D < 1.0 \times 10^{-3}$ mm^2/s (Frac < 1.0) and $D > 3.0 \times 10^{-3}$ mm^2/s (Frac > 3.0) obtained from the statistical model were compared among four groups. Correlation between proposed parameters and conventional apparent diffusion coefficient (ADC) with eGFR was calculated.

Results: There was no significant difference in goodness of fit between the truncated Gaussian and gamma models. Frac < 1.0 and Frac > 3.0 showed good correlation with eGFR, as did ADC. Comparison between groups 1 and 2 showed that only Frac < 1.0 in both distribution models had significant differences.

Conclusion: Statistical models yield robust interpretation of diffusion magnetic resonance (MR) signals with relevance to histological changes in the kidney. The parameters of the statistical models, particularly Frac < 1.0, strongly correlated with eGFR.

Keywords: *chronic kidney disease, estimated glomerular filtration rate, statistical model, magnetic resonance imaging, non-Gaussian diffusion*

Introduction

Pathophysiological changes observed in chronic kidney disease (CKD) include interstitial fibrosis, decreased blood flow, and consequently, ischemia of the tubulointerstitium.[1] Although CKD is a relatively frequent disorder worldwide, the gold standard for diagnosis is the performance of biopsies, while diagnostic imaging remains a challenge. The only established imaging modality for the assessment of renal function is radioisotope scintigraphy. Although scintigraphy allows assessing glomerular filtration rate (GFR)—as an indicator of renal function—of both kidneys separately, it leads to radiation exposure, and does not allow the concurrent assessment of morphological changes.

Magnetic resonance imaging (MRI) has been recently reported as a useful method for the assessment

---

*Corresponding author, Phone: +81-42-995-1689, Fax: +81-42-996-5214, E-mail: shinmoto@ga2.so-net.ne.jp

of pathophysiological changes in impaired kidneys. In particular, diffusion-weighted imaging (DWI) was reported as a potential MRI modality for the evaluation of renal function.[2–6] Several studies have revealed that apparent diffusion coefficient (ADC) of the kidney obtained using the monoexponential model correlates well with the estimated GFR (eGFR).[2,3] In addition, a recent report by Zhao et al. has demonstrated the relation between ADC and eGFR as well as between ADC and histological fibrosis, in CKD patients.[2] However, the ADC approach may be insufficient for describing *in vivo* proton diffusion, because the ADC monoexponential model does not take into account the heterogeneous biological structures that interfere with free diffusion.

The statistical model of Yablonskiy et al. is a non-monoexponential model of DWI, which presumes the continuous distribution of diffusion coefficients within an imaging voxel, potentially providing physiological information, as demonstrated in the human brain.[7,8] They used the truncated Gaussian distribution as a form of diffusion coefficient distribution in their brain studies. However, recently Oshio et al. and Shinmoto et al. reported the application of a statistical model using gamma distribution for prostate cancer.[9,10] In their reports, the histological interpretation of diffusion data seemed possible by introducing the concept of area fractions for diffusion coefficients $D < 1.0 \times 10^{-3}$ mm^2/s and $D > 3.0 \times 10^{-3}$ mm^2/s as parameters that represent restricted diffusion and perfusion, respectively. In this study, we performed DWI examinations using statistical models to assess renal function, with the aim of determining the appropriateness of models with two different distributions (i.e., truncated Gaussian and gamma distributions) for diffusion signal decay in the kidney, and to correlate the parameters obtained from the statistical models with renal function.

Materials and Methods

Patients

This study was approved by the Institutional Clinical Research Ethics Board. Written informed consent was obtained from all participants. In total, 33 patients clinically diagnosed with CKD at our institute were recruited for participation in this study between January 2014 and March 2015. Twenty-one healthy volunteers without renal disorders were also recruited during the same period. Of the 33 patients, three were excluded from the study population because of severe motion artifacts on DWI (n = 1), abnormal high intensity on the left renal cortex (n = 1), and atrophy of the left kidney (n = 1), respectively. The latter two cases were excluded, because the present study was performed on the assumption that the kidney function was bilaterally uniform. An additional patient, who complained of claustrophobia and did not complete MRI examination, was also excluded. Finally, 29 patients (17 men and 12 women; mean age, 65.3 ± 13.0 years) and 21 healthy volunteers (12 men and 9 women; mean age, 49.4 ± 20.1 years) were enrolled. None of the patients had hydronephrosis or underwent nephrectomy.

Serum creatinine levels were measured for all participants. eGFR was calculated using the Modification of Diet in Renal Disease formula, which is recommended by the Japanese Society of Nephrology. The mean of eGFR was 43.3 ± 21.5 ml/min/1.73 m^2 for patients and 85.4 ± 15.3 ml/min/1.73 m^2 for volunteers. The mean interval between blood test and MR examination was 12.8 days for patients and 66.4 days for volunteers. According to the clinical stages of CKD,[11] the study population was divided in four groups based on eGFR (ml/min/1.73 m^2): group 1, eGFR ≥ 90 (normal or high, n = 10); group 2, 60 ≤ eGFR < 90 (mildly decreased, n = 15); group 3, 30 ≤ eGFR < 60 (moderately decreased, n = 17); and group 4, eGFR < 30 (severely decreased or kidney failure, n = 8). A summary of patient characteristics for each group is shown in Table 1.

MRI

All MRI examinations were performed using a 3T MRI scanner (Achieva 3T, Philips Medical Systems, Best, the Netherlands) with a 32-channel phased-array coil. DWI was performed using single-shot echo planar imaging with three orthogonal diffusion sensitization directions, and five b-values (0, 500, 1000, 1500, and

Table 1. Baseline data for the four subject groups

	Group 1	Group 2	Group 3	Group 4
Number of subjects	10	15	17	8
Male	3	9	11	5
Female	7	6	4	3
Age (years)	41.5 ± 14.7	55.1 ± 19.6	67.4 ± 10.2	68.1 ± 16.0
eGFR (ml/min/1.73 m^2)	99.69 ± 1.31	74.4 ± 8.64	46.6 ± 8.96	17.8 ± 8.08

Data are indicated as mean ± standard deviation. eGFR, estimated glomerular filtration rate.
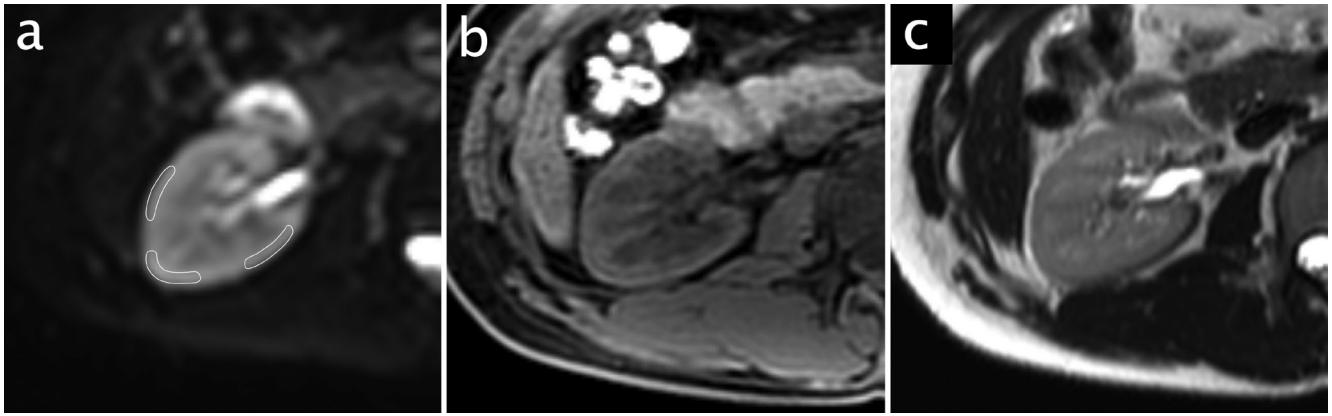
Fig. 1. (**a**) Three regions of interest were placed along the renal cortex on diffusion-weighted images with b-value of 0 (s/mm^2). (**b**, **c**) Anatomical information was obtained from axial T$_1$-weighted images with fat suppression, and axial T$_2$-weighted images.

2000 s/mm^2). DWI was acquired in the transverse plane to cover the entire kidneys bilaterally, with free breathing acquisition. Other parameters were as follows: repetition time (TR)/echo time (TE), 7500/73 ms; scan time, 787.5 s; 5 mm slice thickness with a 0.5 mm gap; motion probing gradient, 3 axes; field of view (FOV), 380 mm × 380 mm; matrix size, 256 × 256; and sensitivity encoding (SENSE), 2. To obtain anatomical information, MR images were acquired using the following parameters: axial and coronal T$_2$-weighted single-shot fast spin-echo (SSFSE) images [TR/TE, infinite/100–152 ms; 5 mm slice thickness without gap; matrix size, 304 × 159 (zero-filled interpolation, ZIP 640), or 320 × 190 (ZIP 512); SENSE, 2]; and axial three-dimensional (3D) fast-field echo T$_1$-weighted images with fat suppression [TR/TE, 2.90–3.07/1.40–1.47 ms; 4 mm (ZIP 2 mm) slice thickness; and matrix size, 252 × 214 (ZIP 400)].

Image analysis

Two experienced radiologists analyzed the MR images. Following a consensus among the radiologists, three regions of interest (ROIs) were placed in the cortex of the right kidney on DWI (b = 0 s/mm^2). Then, signal intensities were measured for each b-value (b = 500, 1000, 1500, and 2000 s/mm^2) using a copy-paste operation. Examples of the ROIs are shown in Fig. 1a. The average of measured signal intensities versus b-value curves was fitted to both the truncated Gaussian and gamma models with a nonlinear least squares method, using the conjugate gradient method.

Equation (1) shows the truncated Gaussian distribution function[7,8]:

$$\rho(D) = A\exp[-(D - D_m)^2/2\sigma^2] \quad (1)$$

where A is the normalization constant, D_m is the distribution maximum, and σ is the width of distribution (only for the condition of $D > 0$).

Equation (2) shows the diffusion signal S when the distribution of D follows the truncated Gaussian distribution function shown in Eq. (1).

$$S(b) = S_0 \frac{1 + \Phi\left(\dfrac{D_m}{\sigma\sqrt{2}} - \dfrac{b\sigma}{\sqrt{2}}\right)}{1 + \Phi\left(\dfrac{D_m}{\sigma\sqrt{2}}\right)} \exp\left(-bD_m + \frac{b^2\sigma^2}{2}\right) \quad (2)$$

where Φ is the error function.

Eq. (3) shows the gamma distribution function[9,11] as follows:

$$\rho(D) = AD^{\alpha-1}\exp(-\beta D) \quad (3)$$

where A is the normalization constant, and α and β are the shape and rate parameters, respectively; while α/β and α/β^2 represent the mean and variance of the gamma distribution, respectively.

Eq. (4) shows the diffusion signal S when the distribution of D follows the gamma distribution function shown in Eq. (3).

$$S(b) = \frac{S_0\beta^\alpha}{(\beta + b)^\alpha} \quad (4)$$

Conventional ADC was determined from two b-values (i.e., 0 and 1000 s/mm^2) using the monoexponential model as a reference.

Signal-to-noise ratio (SNR) of the renal cortex was calculated from DWI at a b-value of 2000 s/mm^2. Since a parallel imaging technique was applied, the mean of the standard deviation (SD) of the signal intensity (SI) in the right erector spinae muscle was used as background noise.[12] The area of ROI for noise was larger than 50 mm^2. SNR calculation is shown in Eq. (5).

$$\text{SNR} = \frac{\text{SI in the renal cortex}}{\begin{array}{l}\text{mean SD of SI in the right erector}\\ \text{spinae muscle}\end{array}} \quad (5)$$
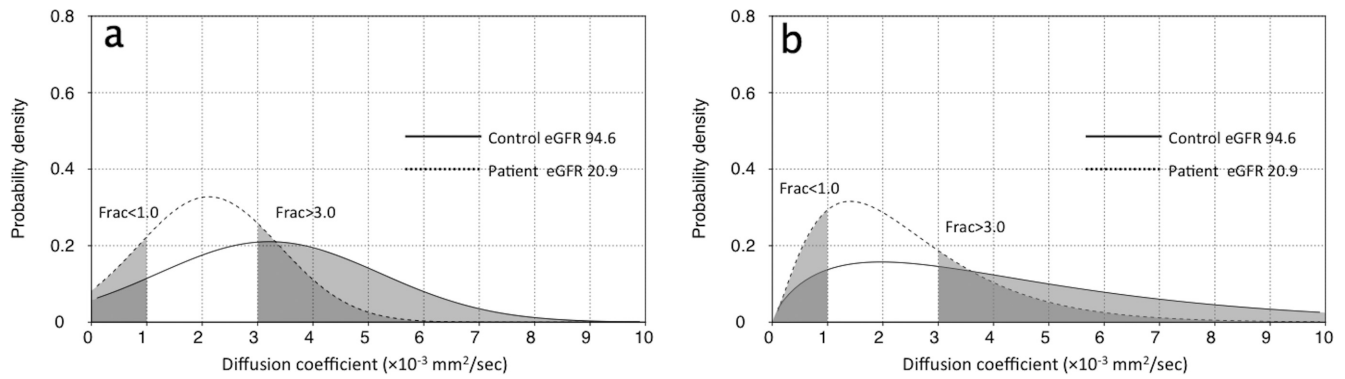
Fig. 2. Probability density functions (PDFs) of the diffusion coefficient (D) in statistical models using truncated Gaussian distribution (**a**), and gamma distribution (**b**). The PDF for a healthy volunteer is shown as a solid curve line, while that for a patient with typical chronic kidney disease (CKD) is shown as a dotted curve line. Distribution of D for the CKD patient is lower than for the healthy volunteer in both models. eGFR, estimated glomerular filtration rate.
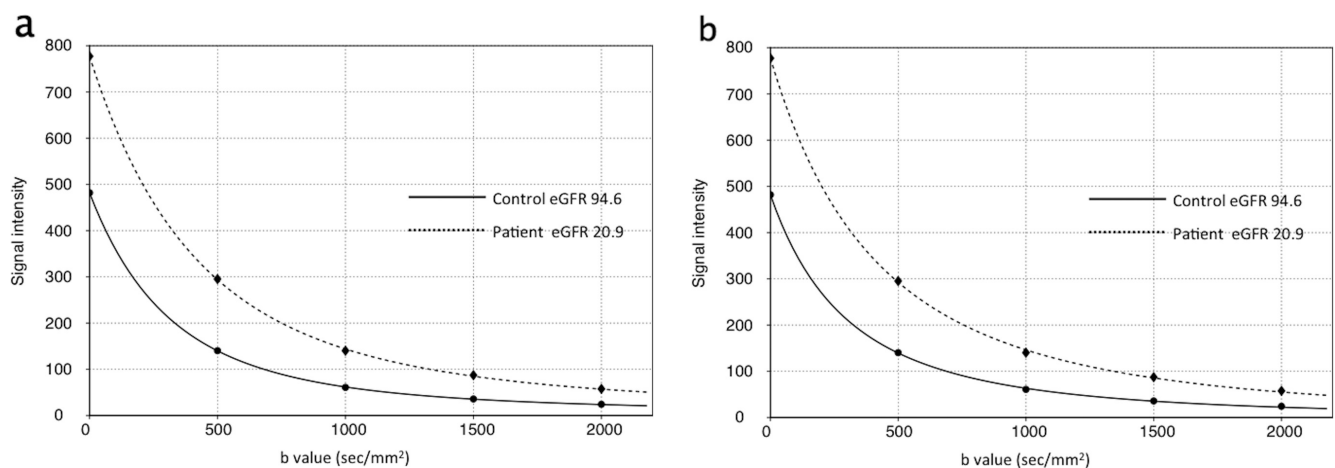
Fig. 3. The graph shows the curve fits for the truncated Gaussian (**a**) and gamma (**b**) models in a healthy volunteer, and a patient with typical chronic kidney disease (CKD). Subjects are the same as in Fig. 2. Curve fitting in each model and for each subject are reasonably good, with negligible differences between the truncated Gaussian and gamma models.

Statistical analysis

The goodness of fit of the truncated Gaussian and gamma models was compared applying the F test using R^2 values for each fit in the entire group and subgroups. The area fractions for $D < 1.0 \times 10^{-3}$ mm²/s (Frac < 1.0), and $D > 3.0 \times 10^{-3}$ mm²/s (Frac > 3.0) in the truncated Gaussian and gamma models, respectively, were determined. Correlation coefficients (r) between ADC and eGFR, and between the proposed area fractions (Frac < 1.0 and Frac > 3.0) and eGFR were calculated in each model using Spearman's rank correlation coefficient. Strength of correlation was interpreted according to Colton's guideline: $0 < |r| < 0.25$, weak or no correlation; $0.25 \leq |r| < 0.50$, fair correlation; $0.50 \leq |r| < 0.75$, moderate correlation; $0.75 \leq |r| \leq 1$, strong correlation.[13]

The parameters obtained from the truncated Gaussian and gamma models, as well as from ADC for groups 2–4 were compared to those of group 1 (eGFR ≥ 90 ml/min/1.73 m²), using the Kruskal-Wallis test with post hoc Steel test.

A P value <0.05 was considered statistically significant in all analyses. The Kruskal-Wallis test with post hoc Steel test was performed using JMP 11 (v11.2.0, SAS Institute Inc., Cary, North Carolina, USA). All other statistical analyses were performed using MedCalc (v11.6.2.0, MedCalc Software, Mariakerke, Belgium).

Results

The mean and SD for ROI size was 51.8 ± 5.35 mm². The mean and SD for SNR with b-value of 2000 s/mm² for renal cortex was 33.7 ± 10.6. Fig. 2 shows the probability density function of D in statistical models using the truncated Gaussian and gamma distributions. The two curves in each distribution model represent the probability density function of D for a typical CKD patient and a healthy volunteer. The distribution of D was lower for CKD patients than for healthy volunteers in each distribution model.

Curve fitting for the truncated Gaussian and gamma models in the same subjects is shown in Fig. 3.

Table 2. Comparison of fitting results between the truncated gaussian and gamma models

	Model	R^2 value	F vs. gamma	P value
Entire group	Truncated Gaussian	0.99992	0.9865	0.47
	Gamma	0.99992	—	—
Group 1	Truncated Gaussian	0.99990	1.4857	0.19
	Gamma	0.99992	—	—
Group 2	Truncated Gaussian	0.99992	0.7354	0.2
	Gamma	0.99990	—	—
Group 3	Truncated Gaussian	0.99994	0.8709	0.35
	Gamma	0.99993	—	—
Group 4	Truncated Gaussian	0.99990	1.2033	0.36
	Gamma	0.99992	—	—

$P < 0.05$ is considered statistically significant after applying the F test using R^2 value.

Table 3. Parameters of statistical models and conventional ADC in each group

	Group 1	Group 2	Group 3	Group 4
eGFR (ml/min/1.73 m^2)	$90 \leq$ eGFR	$60 \leq$ eGFR < 90	$30 \leq$ eGFR < 60	eGFR < 30
Statistical model				
Truncated Gaussian distribution				
Frac <1.0 (%)	7.72 ± 0.75	9.25 ± 0.93*	10.3 ± 1.71*	13.8 ± 1.90*
P	—	<0.01	<0.01	<0.01
Frac >3.0 (%)	56.0 ± 7.29	51.3 ± 3.65	48.56 ± 8.45	33.5 ± 9.56*
P	—	0.31	0.09	<0.01
Gamma distribution				
Frac <1.0 (%)	8.16 ± 1.31	10.1 ± 1.13*	11.3 ± 2.13*	15.6 ± 2.64*
P	—	<0.01	<0.01	<0.01
Frac >3.0 (%)	53.6 ± 6.76	49.3 ± 3.27	47.4 ± 7.61	34.3 ± 7.86*
P	—	0.31	0.18	<0.01
Conventional ADC (×10^{-3} mm^2/s)	2.16 ± 0.13	2.05 ± 0.09	1.97 ± 0.14*	1.71 ± 0.13*
P	—	0.09	<0.01	<0.01

Data are indicated as mean ± standard deviation. $P < 0.05$ is considered statistically significant after applying Kruskal–Wallis test with post hoc Steel test. *$P < 0.05$ versus group 1. ADC, apparent diffusion coefficient; GFR, estimated glomerular filtration rate.

R^2 values for curve fitting in the entire study population were 0.99992 for the truncated Gaussian model, and 0.99992 for the gamma model ($P = 0.47$). The fitting results for the overall study population and for each group are shown in Table 2. Statistical models with both distribution functions provided a reasonably good curve fitting, with no significant differences in the goodness of fit between the two distribution models for the overall population and for each group.

A summary of the parameters obtained from the truncated Gaussian model, the gamma model, and conventional ADC for each group are shown in Table 3. In the truncated Gaussian model, Frac < 1.0 was significantly greater for groups 2 (9.25 ± 0.93%), 3 (10.3 ± 1.71%), and 4 (13.8 ± 1.90%) than for group 1 (7.72 ± 0.75%). Frac > 3.0 was significantly lower for group 4 (33.5 ± 9.56%) than for group 1 (56.0 ± 7.29%), while groups 2 (51.3 ± 3.65%, $P = 0.31$)

and 3 (48.56 ± 8.45%, P = 0.09) showed no significant differences compared to group 1 (56.0 ± 7.29%).

Statistical analysis for the gamma model showed similar results. Frac < 1.0 was significantly greater for groups 2 (10.1 ± 1.13%), 3 (11.3 ± 2.13%), and 4 (15.6 ± 2.64%) than for group 1 (8.16 ± 1.31%). Frac > 3.0 was significantly lower only for group 4 (34.3 ± 7.86%) compared to group 1 (53.6 ± 6.76 %).

ADC was significantly lower for groups 3 (1.97 ± 0.14 × 10^{-3} mm^2/s) and 4 (1.71 ± 0.13 × 10^{-3} mm^2/s) than for group 1 (2.16 ± 0.13 × 10^{-3} mm^2/s); while group 2 (2.05 ± 0.09 × 10^{-3} mm^2/s, P = 0.09) showed no statistical significant differences.

The relations between parameters in each model and eGFR are shown in Fig. 4. All parameters showed a significant correlation ($P < 0.05$) with eGFR. In particular, a strong correlation was found for Frac < 1.0
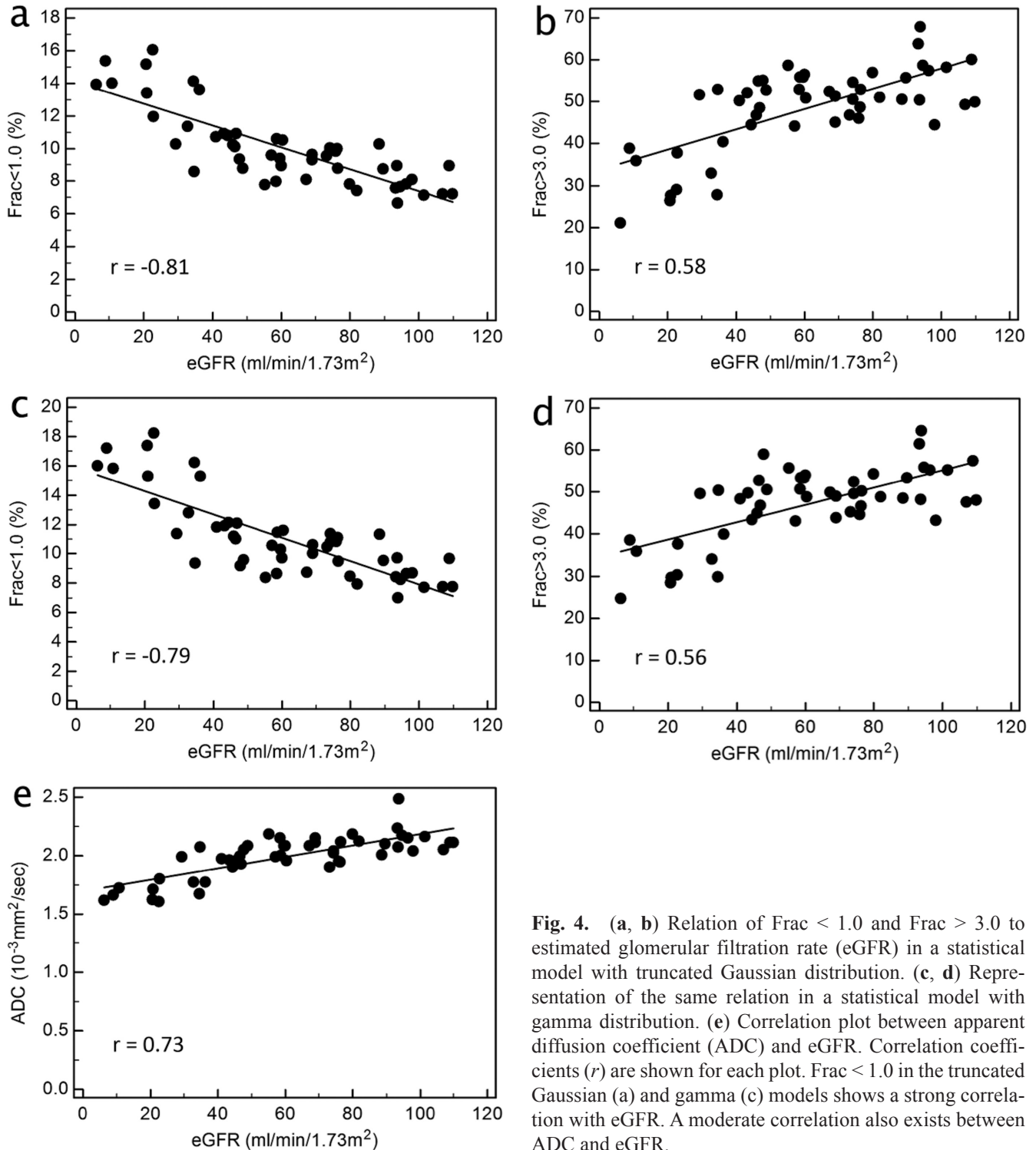
Fig. 4. (**a**, **b**) Relation of Frac < 1.0 and Frac > 3.0 to estimated glomerular filtration rate (eGFR) in a statistical model with truncated Gaussian distribution. (**c**, **d**) Representation of the same relation in a statistical model with gamma distribution. (**e**) Correlation plot between apparent diffusion coefficient (ADC) and eGFR. Correlation coefficients (r) are shown for each plot. Frac < 1.0 in the truncated Gaussian (a) and gamma (c) models shows a strong correlation with eGFR. A moderate correlation also exists between ADC and eGFR.

in both distribution models. Although ADC obtained from the monoexponential model also showed a moderate positive correlation ($r = 0.73$), Frac < 1.0 showed a trend towards a strong negative correlation with eGFR, which was stronger than that with ADC (truncated Gaussian model, $r = -0.81$; gamma model, $r = -0.79$).

Discussion

The statistical model of Yablonskiy et al. is a non-monoexponential model of DWI that was first applied to the brain.[7,8] Until recently, there were few studies on DWI using statistical models. However, Oshio et al. recently applied statistical models using gamma distribution for prostate cancer, and introduced the concept of area fractions for $D < 1.0 \times 10^{-3}$ mm²/s (Frac < 1.0) and $D > 3.0 \times 10^{-3}$ mm²/s (Frac > 3.0), as parameters representing restricted diffusion and perfusion, respectively.[9,10] In the current study we have found that both Frac < 1.0 and Frac > 3.0 had strong and moderate correlation with eGFR, respectively.

Zhao et al. reported that ADC for the renal cortex showed a significant correlation with histopathological fibrosis scores and eGFR.[2] The relation between ADC and renal fibrosis in a murine model was also reported by Togao et al.[14] According to their report, ADC can be an efficient parameter for monitoring the progression of renal fibrosis.[14] They also suggested that the predominant cause of lower ADC in fibrotic kidneys is a higher density of cells, including myofibroblasts present in the interstitial space, as typically observed during renal fibrogenesis.[14] Deposition of collagen fibers is also considered a possible cause that interferes with the Brownian motion of water, although this remains controversial.[15–18] Therefore, when statistical models are applied for the analysis of DWI findings for the kidney, Frac < 1.0 could be considered an index of fibrosis in the impaired kidney.

To our knowledge, the present study is the first report on DWI of the kidney using statistical models in patients with CKD. Care should be taken to not confuse the distribution functions of D proposed by statistical models, with ADC histogram analysis. Histogram analysis of ADC is a simple voxel-based analysis that uses a frequency distribution chart, and assumes specific ADC values in each voxel. On the other hand, statistical models are non-monoexponential models of DWI that presume continuous distribution of D within an imaging voxel, and are not a mere chart analysis. Therefore, the curves shown in Fig. 2 are not frequency distribution charts, but probability density functions of D, led by Eqs. (1) and (3).

In this study, fitting results for the two statistical models (i.e., truncated Gaussian and gamma models)

showed a notable good fit with the diffusion signal decay in the renal cortex. There was no significant difference in the goodness of fit between these two models in the present study. Previous studies have shown that the gamma model offered a better fit in prostate cancer compared to the truncated Gaussian model.[9,10] However, Shinmoto et al. described that there were no significant differences in curve fitting between the truncated Gaussian and gamma models in benign prostatic hypertrophy and the healthy peripheral zone of the prostate.[10] The reason for this difference was hypothesized in that the distribution of D in prostate cancer was strongly skewed toward the lower D values compared to benign prostatic hypertrophy and the healthy peripheral zone.[10] Our results can also be understood in terms of the distribution of D. This is, the distributions of D in healthy and impaired kidneys might be relatively even or skewed toward lower D values, but not as much as in prostate cancer.

Various MRI techniques, including DWI with monoexponential and intravoxel incoherent motion (IVIM) models, diffusion tensor imaging, blood oxygen level-dependent MRI, and arterial spin labeling have been reported as noninvasive approaches for the evaluation of renal function.[2–6,19–21] In particular, ADC has been widely used in functional MRI of the kidney.[2–4] As mentioned previously, a recent report by Zhao et al. revealed that renal ADC values strongly correlated with eGFR and histological measures of fibrosis.[2] In addition to the monoexponential model, Ichikawa et al. described the relation between eGFR and parameters calculated using the IVIM model.[5] They reported that as renal dysfunction progresses, fast diffusion component (i.e., perfusion component) may be decreased at an earlier stage compared to slow diffusion components in the renal cortex. In contrast, the present study showed that only Frac < 1.0, which represents restricted diffusion, presented significant differences between group 1 (i.e., normal kidney function) and group 2 (i.e., slightly impaired eGFR), which means that Frac < 1.0 was the most sensitive to an early decline in renal function compared to Frac > 3.0 (i.e., perfusion component) and ADC. Although, the results of the previous research using the IVIM model by Ichikawa et al.[5] and that of the present study using the statistical model vary, the specific reason for this difference is still unclear, and further research and analysis will be needed.

Physiological processes other than perfusion, such as urine flow, occur in the renal tubule. Although urine flow in the renal tubule may slightly contribute to Frac > 3.0, considering the volume of urine flow versus that of renal artery blood flow, Frac > 3.0 is deemed to be affected mainly by perfusion. According to recent MR research by Khatir et al., the renal blood flow of the whole kidney was reduced in CKD patients compared

to the healthy controls; however, there was no significant difference between the renal blood flow per kidney volume (i.e., volume corrected renal blood flow) for both CKD patients and healthy controls.[22] In the present study, Frac > 3.0, which represents perfusion per voxel, was relatively even until eGFR of 40 ml/min/1.73 m[2] and decreased only in patients with severe CKD (Fig. 4b, d). Therefore, our results of Frac > 3.0, which has a relatively weak correlation with eGFR compared to Frac < 1.0, are largely consistent with the results of the previous study by Khatir et al.[22] On the other hand, the ADC value is affected not only by restricted diffusion (i.e., fibrosis) but also by the fast diffusion component (i.e., perfusion). Consequently, Frac < 1.0 can be considered a better indicator in terms of independency from the fast diffusion component.

Meanwhile, although IVIM is an informative DWI model with biexponential function that can be applied to various organs, reliable biexponential fitting is considered difficult because of associated mathematical fragility.[23–25] Statistical models using truncated Gaussian and gamma distributions have two free parameters each; therefore, parameter calculation is more reliable than with the biexponential model, which has three free parameters. Taken together, statistical models are considered a robust approach for the analysis of diffusion signals, and may provide separate information for fibrosis and kidney perfusion.

The statistical model may provide information of renal fibrosis and perfusion in terms of Frac < 1.0 and Frac > 3.0 whereas the monoexponential model dose not. While Frac < 1.0 from DWI by using the statistical model detects early change in CKD and shows better correlation with eGFR (i.e., renal function) than does conventional ADC, and is a potential split renal function test with concurrent morphological assessment, the eGFR obtained with blood test cannot assess split renal function. Moreover, that DWI is performed without any radiation exposure is an additional advantage over radioisotope renal scintigraphy.

The present study has several limitations. First, this study was performed at a single institution, and had a relatively small number of subjects. Second, it analyzed the signal from the renal cortex alone; analysis of the medulla could not be performed because the corticomedullary junction was ill-defined, and determination of the area of the medulla in advanced CKD patients was difficult. Third, the interval between blood test and MR examination was relatively long, especially in the healthy volunteers (mean, 66.4 days). However, eGFR or renal function is considered stable among healthy individuals. In addition, we only included cases of stable CKD and not acute renal failure; therefore, there was little change in the renal function of our patients in the given time interval (mean, 12.8 days). Finally,

pathological diagnosis was not performed because few patients underwent renal biopsy. Most patients were diagnosed with CKD on the basis of clinical information without invasive biopsy; therefore, the relation between parameters obtained from the statistical models and pathological findings remain unclear in the present study.

In conclusion, the parameters obtained with DWI using statistical models with truncated Gaussian and gamma distributions in this study, particularly Frac < 1.0, showed a strong correlation with renal function. The results suggest that statistical models are robust and feasible for the interpretation of diffusion MR signal decays with relevance to histological changes in the kidney.

References

1. Nangaku M. Chronic hypoxia and tubulointerstitial injury: a final common pathway to end-stage renal failure. J Am Soc Nephrol 2006; 17:17–25.
2. Zhao J, Wang ZJ, Liu M, et al. Assessment of renal fibrosis in chronic kidney disease using diffusion-weighted MRI. Clin Radiol 2014; 69:1117–1122.
3. Toya R, Naganawa S, Kawai H, Ikeda M. Correlation between estimated glomerular filtration rate (eGFR) and apparent diffusion coefficient (ADC) values of the kidneys. Magn Reson Med Sci 2010; 9:59–64.
4. Inoue T, Kozawa H, Okada H, et al. Noninvasive evaluation of kidney hypoxia and fibrosis using magnetic resonance imaging. J Am Soc Nephrol 2011; 22:1429–1434.
5. Ichikawa S, Motosugi U, Ichikawa T, Sano K, Morisaka H, Araki T. Intravoxel incoherent motion imaging of the kidney: alternations in diffusion and perfusion in patients with renal dysfunction. Magn Reson Imaging 2013; 31:414–417.
6. Ebrahimi B, Rihal N, Woollard JR, Krier JD, Eirin A, Lerman LO. Assessment of renal artery stenosis using intravoxel incoherent motion diffusion-weighted magnetic resonance imaging analysis. Invest Radiol 2014; 49:640–646.
7. Yablonskiy DA, Bretthorst GL, Ackerman JJ. Statistical model for diffusion attenuated MR signal. Magn Reson Med 2003; 50:664–669.
8. Yablonskiy DA, Sukstanskii AL. Theoretical models of the diffusion weighted MR signal. NMR Biomed 2010; 23:661–681.
9. Oshio K, Shinmoto H, Mulkern RV. Interpretation of diffusion MR imaging data using a gamma distribution model. Magn Reson Med Sci 2014; 13:191–195.
10. Shinmoto H, Oshio K, Tamura C, et al. Diffusion-weighted imaging of prostate cancer using a statistical model based on the gamma distribution. J Magn Reson Imaging 2015; 42:56–62.
11. KDIGO CKD Work Group. KDIGO 2012 clinical practice guideline for the evaluation and management of chronic kidney disease. Kidney Int Suppl 2013; 3:1–150.

12. Heverhagen JT. Noise measurement and estimation in MR imaging experiments. Radiology 2007; 245:638–639.

13. Colton T. Statistics in Medicine. Boston, MA: Little, Brown and Company, 1974; 211.

14. Togao O, Doi S, Kuro-o M, Masaki T, Yorioka N, Takahashi M. Assessment of renal fibrosis with diffusion-weighted MR imaging: study with murine model of unilateral ureteral obstruction. Radiology 2010; 255:772−780.

15. Lu PX, Huang H, Yuan J, et al. Decreases in molecular diffusion, perfusion fraction and perfusion-related diffusion in fibrotic livers: a prospective clinical intravoxel incoherent motion MRI imaging study. PLoS One 2014; 9:e113846.

16. Luciani A, Vignaud A, Cavet M, et al. Liver cirrhosis: intravoxel incoherent motion MR imaging—pilot study. Radiology 2008; 249:891–899.

17. Annet L, Peeters F, Abarca-Quinones J, Leclercq I, Moulin P, Van Beers BE. Assessment of diffusion-weighted MR imaging in liver fibrosis. J Magn Reson Imaging 2007; 25:122–128.

18. Taouli B, Tolia AJ, Losada M, et al. Diffusion-weighted MRI for quantification of liver fibrosis: preliminary experience. AJR Am J Roentgenol 2007; 189:799–806.

19. Liu Z, Xu Y, Zhang J, et al. Chronic kidney disease: pathological and functional assessment with diffusion tensor imaging at 3 T MR. Eur Radiol 2015; 25:652–660.

20. Heusch P, Wittsack HJ, Blondin D, et al. Functional evaluation of transplanted kidneys using arterial spin labeling MRI. J Magn Reson Imaging 2014; 40:84–89.

21. Zhang JL, Rusinek H, Chandarana H, Lee VS. Functional MRI of the kidneys. J Magn Reson Imaging 2013; 37:282–293.

22. Khatir DS, Pedersen M, Jespersen B, Buus NH. Evaluation of renal blood flow and oxygenation in CKD using magnetic resonance imaging. Am J Kidney Dis 2015; 66: 402–411.

23. Oshio K. Reliability of bi-exponential parameter estimation. In: Proceedings of the 20th Annual Meeting ISMRM, Melbourne, 2012 (abstract 3583).

24. Acton FS. Numerical Methods that Work, 2nd printing. Washington, DC: The Mathematical Association of America, 1990; 253.

25. Mulkern RV, Haker SJ, Maier SE. On high b diffusion imaging in the human brain: ruminations and experimental insights. Magn Reson Imaging 2009; 27:1151–1162.